ORNL/TM-2023/2985

UCO TRISO MiniFuel FY23 NSUF-Kairos Power Post-Irradiation Examination Status Report

A.G. Le Coq
C.M. Petrie
J.M. Harp
T.J. Gerczak
K.D. Linton
R. Latta (Kairos Power)

August 2023

M3UA-22OR0702012

OAK RIDGE National Laboratory

ORNL IS MANAGED BY UT-BATTELLE LLC FOR THE US DEPARTMENT OF ENERGY

ORNL/TM-2023/2985

Nuclear Science User Facilities

UCO TRISO MINIFUEL FY23 NSUF-KAIROS POWER POST-IRRADIATION EXAMINATION STATUS REPORT

A.G. Le Coq
C.M. Petrie
J.M. Harp
T.J. Gerczak
K.D. Linton
R. Latta (Kairos Power)

August 2023

Prepared by
OAK RIDGE NATIONAL LABORATORY
Oak Ridge, TN 37831
managed by
UT-BATTELLE LLC
for the
US DEPARTMENT OF ENERGY
under contract DE-AC05-00OR22725

CONTENTS

ABSTRACT

Irradiation of miniature tristructural isotropic (TRISO)–coated particle fuel compacts at high-power particle was performed in the Oak Ridge National Laboratory's (ORNL's) High Flux Isotope Reactor (HFIR) using the MiniFuel irradiation capability. Each compact comprised 20 TRISO particles with a low-enriched uranium carbide uranium oxide (UCO), natural UCO, or low-enriched UO_2 kernel within a graphitic matrix. After irradiation, the MiniFuel targets and subcapsules were disassembled to recover the irradiated fuel specimens and pursue post-irradiation examination (PIE) to inform Kairos Power on the fuel specimen performance. This report describes the PIE results collected to date, including dilatometry on the passive thermometry to confirm the irradiation temperature, fission gas release measurements, and gamma counting. This work was funded by the Nuclear Science User Facilities program.

ABBREVIATIONS

BU	burnup
DLBL	deconsolidation leach burn leach
EOI	end of irradiation
FGR	fission gas release
FHR	fluoride salt-cooled high-temperature reactor
FIMA	fission per initial metal atom
FP	fission product
HFIR	High Flux Isotope Reactor
IFEL	Irradiated Fuels Examination Laboratory
IMGA	Irradiated Microsphere Gamma Analyzer
KP	Kairos Power
LAMDA	Low-Activation Material Development and Analysis
LEUCO	low-enriched uranium carbide uranium oxide
MDA	minimum detectable activity
NSUF	Nuclear Science User Facilities
NUCO	natural uranium carbide uranium oxide
ORNL	Oak Ridge National Laboratory
PIE	post-irradiation examination
R-A-S	radial-axial-subcapsule
SiC	silicon carbide
TM	thermometry
TRISO	tristructural isotropic
VXF	vertical experiment facility
XCT	x-ray computed tomography

LIST OF FIGURES

LIST OF TABLES

1. INTRODUCTION

To support the development and application of tristructural isotropic (TRISO) fuels in advanced reactors, including Kairos Power's (KP's) fluoride salt–cooled high-temperature reactor (FHR), irradiation testing of TRISO-bearing fuel compacts has been performed at Oak Ridge National Laboratory (ORNL). The fuel compacts were fabricated at ORNL using natural uranium carbide uranium oxide (NUCO), low-enriched uranium carbide uranium oxide (LEUCO), or UO_2 TRISO particles in a graphite matrix, each compact containing 20 TRISO particles [1]. The goal of this experiment is to study the performance of TRISO fuel compacts under prototypical KP-FHR conditions—that is, at higher particle power (>20 MW/m^3) and lower operating temperatures (e.g., down to 500°C) than those of high-temperature gas reactor concepts.

The MiniFuel irradiation capability [2] was used for irradiation of the fuel compacts in a vertical experiment facility (VXF) in ORNL's High Flux Isotope Reactor (HFIR). The experimental design is detailed in Gallagher et al. [3], and the irradiation vehicle is represented in Figure 1 [4]. Each MiniFuel subcapsule contains one fuel compact. The fuel compact is placed between SiC spacers to minimize interaction of the graphite matrix with the surrounding molybdenum subcapsule components. A graphite disk, also referred to as fission product (FP) sink, is placed at the top of the subcapsules to capture potential FP released into the subcapsule. A silicon carbide (SiC) passive thermometry (TM) instrument is present in each subcapsule and is used after irradiation to confirm the experiment irradiation temperature. Five MiniFuel targets were assembled, as described in Le Coq et al. [5].

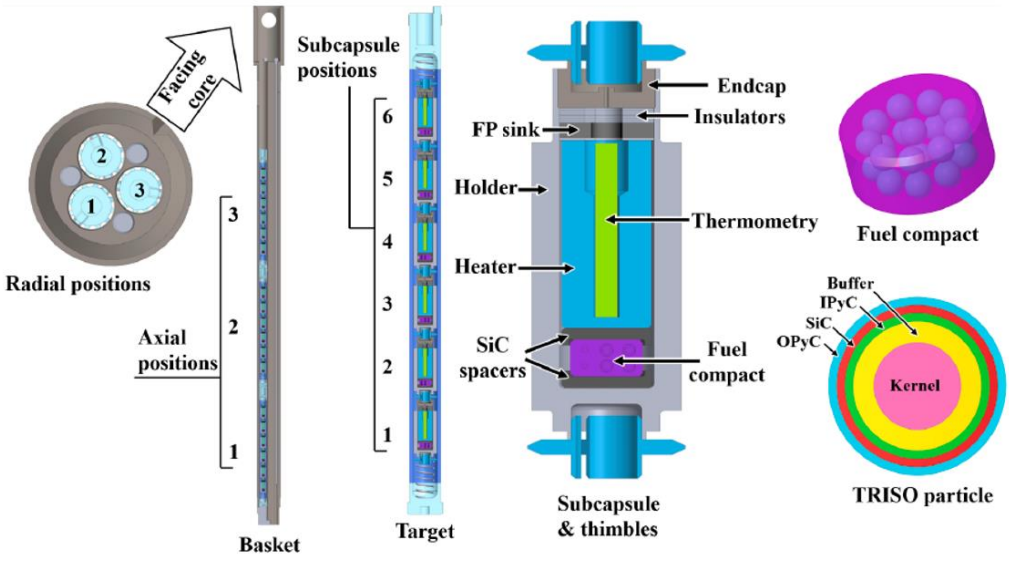

Figure 1. Schematic of VXF MiniFuel vehicle and internal components [4].

The start of the post-irradiation campaign, the target disassembly, is recorded in a previous status report [6]. This report describes the subsequent post-irradiation examination (PIE) results collected to date on the KP MiniFuel targets. Table 1 presents the subcapsule details for each target: the time- and volume-averaged SiC layers' target irradiation temperature, the subcapsule IDs, the irradiation position in the MiniFuel irradiation basket, the type and ID of the fuel compacts, and the discharge burnup predicted by numerical calculations [4]. One should note that the subcapsule ID does not always match the radial-axial-subcapsule (R-A-S) irradiation position in the MiniFuel basket. Each target contains fuel compacts of the same type and with similar irradiation conditions to offer redundancy and provide several data points on the fuel

performance. The results in this report are presented for each subcapsule using the subcapsule IDs in Table 1.

Table 1. KP targets, subcapsules, and specimen details.

Target ID	Target irradiation temperature (°C)	Subcapsule ID	Fuel compact	R-A-S position	Specimen ID	Predicted burnup (%FIMA)
KP01	900	KP121	LEUCO	1-2-1	LEU09-M01E	11.70
		KP122	UO_2	1-2-2	LEU11-M01B	8.55
		KP123	LEUCO	1-2-3	LEU09-M07E	11.92
		KP124	UO_2	1-2-4	LEU11-M05B	8.62
		KP125	LEUCO	1-2-5	LEU09-M09E	11.89
		KP126	UO_2	1-2-6	LEU11-M14B	8.51
KP02	500	KP221	LEUCO	3-2-1	LEU09-M10E	12.24
		KP222	NUCO	3-2-2	NUCO425-08T-M02F	1.86
		KP223	LEUCO	3-2-3	LEU09-M14E	12.43
		KP224	NUCO	3-2-4	NUCO425-08T-M03F	1.90
		KP225	LEUCO	3-2-5	LEU09-M16E	12.41
		KP226	NUCO	3-2-6	NUCO425-08T-M04F	1.83
KP03	500	KP231	LEUCO	3-3-1	LEU09-M17E	11.44
		KP232	LEUCO	3-3-2	LEU09-M19E	10.99
		KP233	LEUCO	3-3-3	LEU09-M21E	10.47
		KP234	LEUCO	3-3-4	LEU09-M22E	9.88
		KP235	LEUCO	3-3-5	LEU09-M24E	9.18
		KP236	LEUCO	3-3-6	LEU09-M25E	8.42
KP04	700	KP321	LEUCO	2-2-1	LEU09-M26E	12.21
		KP322	NUCO	2-2-2	NUCO425-08T-M05F	1.85
		KP323	LEUCO	2-2-3	LEU09-M29E	12.42
		KP324	NUCO	2-2-4	NUCO425-08T-M07F	1.89
		KP325	LEUCO	2-2-5	LEU09-M32E	12.39
		KP326	NUCO	2-2-6	NUCO425-08T-M08F	1.83
KP05	700	KP331	LEUCO	2-3-1	LEU09-M34E	11.45
		KP332	LEUCO	2-3-2	LEU09-M35E	11.00
		KP333	LEUCO	2-3-3	LEU09-M36E	10.50
		KP334	LEUCO	2-3-4	LEU09-M38E	9.90
		KP335	LEUCO	2-3-5	LEU09-M39E	9.22
		KP336	LEUCO	2-3-6	LEU09-M42E	8.45

2. SUBCAPSULE DISASSEMBLY

After target disassembly [6] at the Irradiated Fuels Examination Laboratory (IFEL), the recovered subcapsules were queued for puncturing to collect fission gas release (FGR) measurements prior to subcapsule disassembly. The FGR results are discussed in Section 4.1. To date, six subcapsules (KP224, KP223, KP124, KP123, KP324, KP323) were disassembled to recover the internal components of interest, such as the passive SiC TM and the fuel compact. Each subcapsule was set on a low-speed saw to perform a cut at the top of the subcapsule. The location of the cut was estimated from the holder shoulder to be slightly above the FP sink. In some cases, the FGR puncturing damaged the wall of the subcapsule, forcing it inward and preventing the extraction of any subcapsule internal components. For these cases, a second cut was performed at the top of the subcapsule below the puncturing hole, sacrificing the FP sink. Figure 2 shows various steps of the subcapsule disassembly. Subcapsule KP323 was significantly damaged by the puncturing during disassembly, as shown in Figure 3: the end cap was dislodged by the puncturing. A cut at the top of the subcapsule was still required to extract the subcapsule internal components.

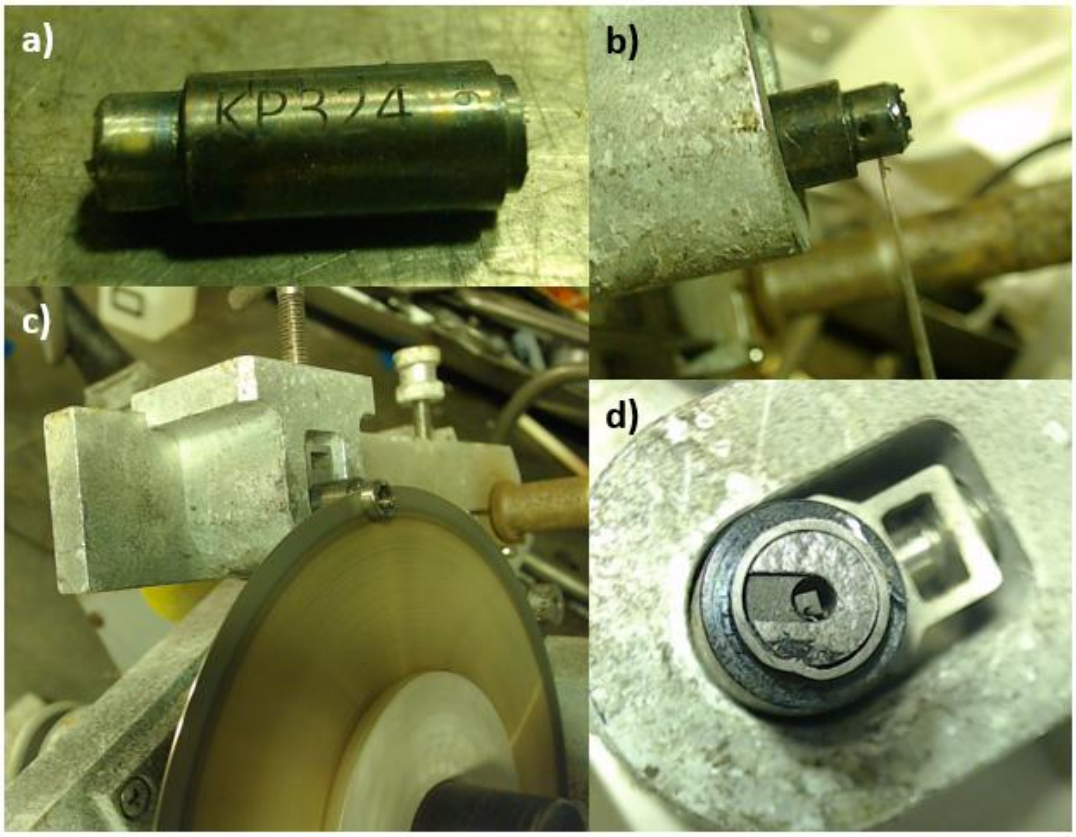

Figure 2. Subcapsule disassembly pictures. a) identification of the subcapsule prior to disassembly, b) subcapsule set on the low-speed saw to perform a cut at the top of the part, c) subcapsule being cut, and d) subcapsule cut open revealing a grafoil disk and the top of the SiC TM.

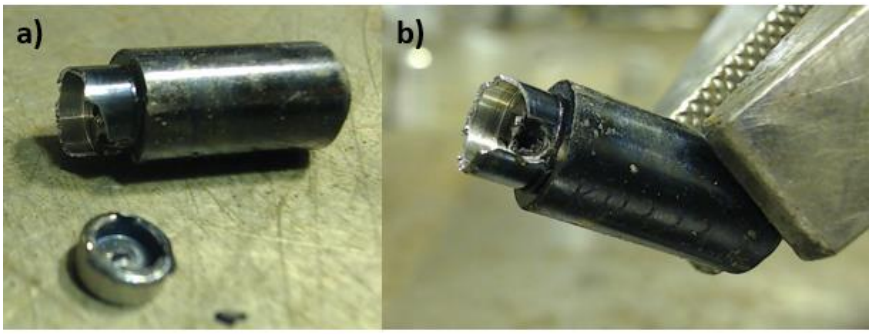

Figure 3. Subcapsule KP323 after puncturing and before disassembly. a) end cap dislodged from the holder, and b) top of the holder damaged from puncturing.

The SiC TM was recovered from all six disassembled subcapsules and was transferred to the Low-Activation Materials Development and Analysis (LAMDA) laboratory for analysis (see Section 3). The FP sink was either fully or partially recovered for four of the six disassembled subcapsules, and the two spacers were set aside for one subcapsule for which no FP sink was recovered. Figure 4 shows the fuel specimens recovered from the six subcapsules after disassembly and after transfer to the Irradiated Microsphere Gamma Analyzer (IMGA) cell. Three compacts were recovered intact (KP324, KP224, KP223), including one compact (KP223) showing cracks in the matrix. One compact (KP323) was recovered significantly cracked after disassembly and was finally broken into pieces after transfer to IMGA. Two compacts (KP124 and KP123) showed a powderized graphite matrix upon disassembly. A total of 19 and 18 particles were recovered for these compacts, respectively. The IMGA image of the KP124 particles in Figure 4 also displays five 500 μm pin balls for scale. All particles recovered seem to have a diameter corresponding to the mean average TRISO particle size of 953 μm [7]. The lack of an intact graphite matrix upon disassembly does not necessarily mean that the corresponding compact's fuel particles have failed. The leaching step to be performed, discussed in Section 6, will include chemical analysis of available uranium in solution, which would indicate failure of a TRISO particle. It is not clear whether the damage to the compact occurred during irradiation, post-irradiation handling, or disassembly. Both KP124 and KP123 were targeted for high-temperature irradiation, which may have contributed to these compacts' greater friability. Additionally, it should be noted that the compacting used in this experiment was primarily meant to conduct heat away from the TRISO particles to achieve the desired irradiation conditions. The compacting technique used in this work was experimental, on the low end but within the bounds of matrix densities explored in the AGR irradiation experiments [1], and not meant to create a structurally sound component.

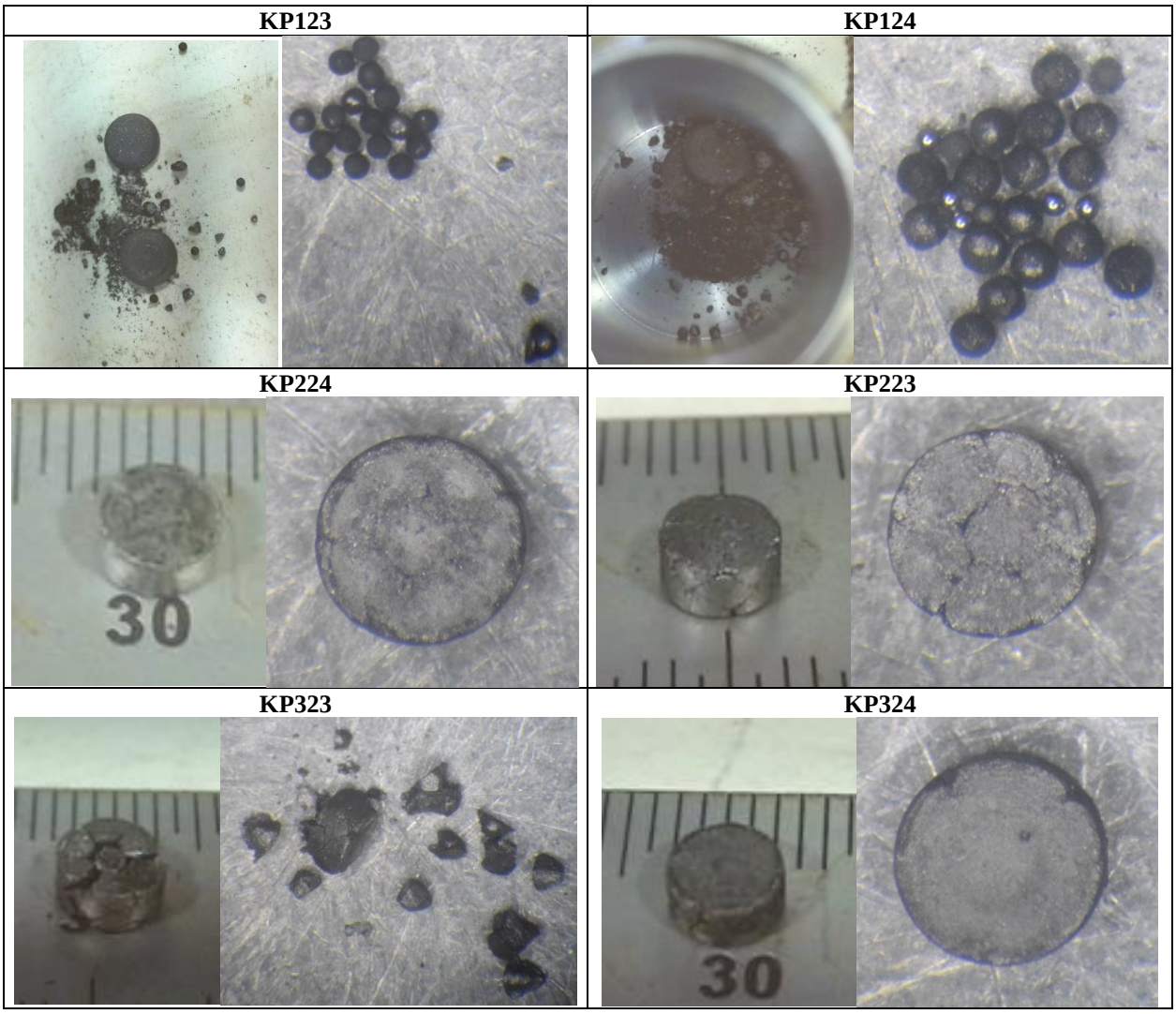

Figure 4. Fuel specimens recovered from the six disassembled subcapsules. For each subcapsule, the picture on the left shows the fuel specimen immediately after disassembly, and the picture on the right shows the specimens after transfer to IMGA.

3. THERMOMETRY ANALYSIS

The six passive SiC TMs were analyzed in LAMDA via dilatometry [8] to confirm the corresponding subcapsules irradiation temperature. The average TM temperature obtained via dilatometry was compared to the predicted average TM temperature at the end of irradiation (EOI) from the as-built as-irradiated numerical calculations (see Table 7 in Gorton et al. [4]). Figure 5 shows the corresponding results. Overall, the experimental TM temperatures are in agreement with the predicted TM temperatures. The difference between experimental and predicted temperature increases with the target temperature: a difference of 2%, 9%, and 13% was observed for target temperatures of 500°C (KP02 target), 700°C (KP04 target), and 900°C (KP01), respectively. For the higher target temperatures, the experimental temperatures are lower than the predicted ones. The average kernel and SiC layer temperatures over the length of the irradiation were estimated from the dilatometry results and the predicted average temperature of the components [6]. The results are summarized in Table 2.

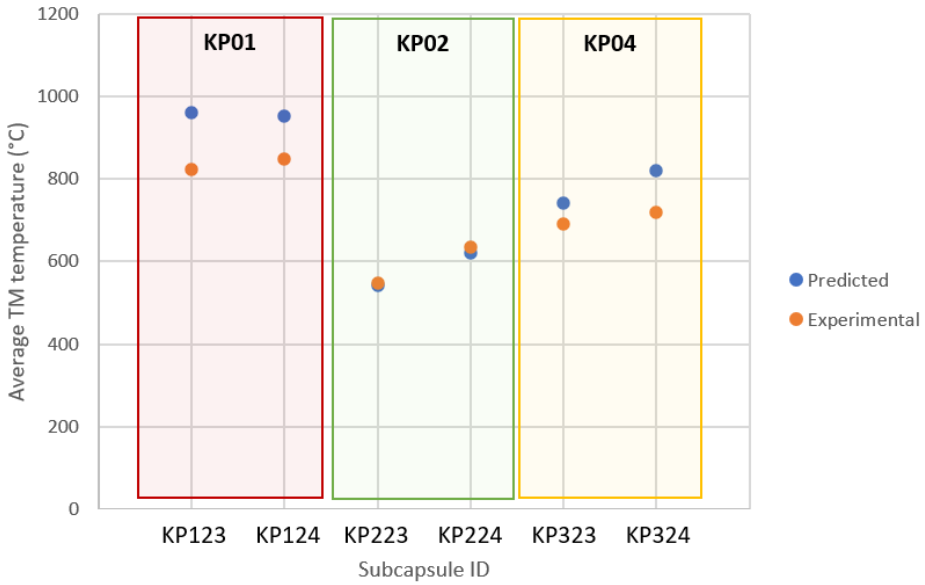

Figure 5. Predicted and experimental average TM temperature for the six disassembled subcapsules.

Table 2. Predicted and experimental TM, kernel, and SiC layer temperatures.

Subcapsule ID	Predicted temperatures (°C)				Experimental temperatures (°C)		
	TM (EOI)	TM (average)	Kernel (average)	SiC layer (average)	TM (dilatometry)	Kernel (average)	SiC layer (average)
KP123	961.4	987.8	1005 .0	993.4	824.1	867.7	856.1
KP124	953.1	980.4	1003.3	990.7	850.2	900.4	887.8
KP223	541.8	555.5	585.6	572.7	547.0	590.8	577.9
KP224	620.3	612.4	597.3	595.4	635.6	612.6	610.7
KP323	741.2	760.4	783.9	771.5	690.1	732.8	720.4
KP324	819.5	814.7	796.3	794.5	720.8	697.6	695.8

4. COMPACTS POST-IRRADIATION EXAMINATION

4.1 FISSION GAS RELEASE MEASUREMENTS

Thirteen subcapsules have been punctured to date using IFEL's puncture system to measure FGR. The puncturing system allows analysts to sweep the gas present in the subcapsule into cold traps. The cold traps are then measured with a high-purity germanium detector for a minimum of six hours to determine the activity of Kr-85 released from the subcapsule. Finally, the Kr-85 release activity is compared with the predicted total activity of Kr-85 present in the subcapsule at EOI. More information on the puncture system can be found in Harp et al. [9].

Table 3 presents the FGR results for the thirteen punctured subcapsules. The total calculated Kr-85 activity represents the predicted Kr-85 at EOI from the as-built, as-irradiated calculation, whereas the released Kr-85 activity represents the measured Kr-85 activity from the puncture, decay-corrected to the EOI. The FGR results are compared to the recoil release from a single failed particle calculated from Lewis [10]. The recoil release calculations used recoil ranges determined from the Stopping Range in Matter (SRIM) code, and as-fabricated fuel dimensions, compositions, densities, and enrichments were used as inputs. All

calculations assumed 108 MeV Kr-85 ions, which were determined to have ranges of ~8.5–8.8 µm, depending on the specific fuel kernel. The calculated recoil release provides a lower bound for the fission gas inventory than might be expected if a single particle were to fail with a pathway to release to the plenum region of the subcapsule. Thus, the calculated recoil release is helpful to understand whether the measured FGR might indicate the possibility of failed TRISO particles. Subcapsules KP323 and KP126 were unsuccessfully punctured: the puncture pin insertion led to a significant deformation of the holder wall, and the top of the subcapsule was sheared off (see example in Figure 3). Subcapsule KP226 was successfully punctured, and no Kr-85 was detected in the traps. However, the spectra were accidentally not recorded, and thus no minimum detectable activity (MDA) value is available. Most of the subcapsules show a Kr-85 release activity under the MDA; Table 3 presents the measured FGR upper bound for these cases, which is below the expected recoil release and thus suggests no particle failure. Three subcapsules show a measurable Kr-85 activity from the puncturing. Subcapsule KP124 shows a FGR more than twice the recoil release from a single failed particle, suggesting a potential particle failure for this fuel specimen. The leaching measurements to be performed (see Section 6) will confirm the number of failed particles for each fuel specimen.

Table 3. FGR results collected to date.

Subcapsule ID	Total calculated Kr-85 activity (µCi)	Released Kr-85 activity (µCi)	Rel. uncertainty	FGR	Recoil release from a single failed particle
KP121	3.37E+02	< 4.23E-02		**< 0.01%**	0.15%
KP122	3.90E+02	< 8.21E-03		**< 0.00%**	0.13%
KP123	3.42E+02	< 7.15E-02		**< 0.02%**	0.15%
KP124	3.93E+02	1.35E+00	8%	**0.34% ± 0.03%**	0.13%
KP125	3.41E+02	< 9.92E-03		**< 0.00%**	0.15%
KP126	3.88E+02	Issue with puncturing		**N/A**	0.13%
KP222	3.22E+01	< 5.16E-02		**< 0.16%**	0.16%
KP223	3.53E+02	< 8.09E-02		**< 0.02%**	0.15%
KP224	3.27E+01	5.03E-02	14%	**0.15% ± 0.02%**	0.16%
KP225	3.53E+02	< 5.20E-02		**< 0.01%**	0.15%
KP226	3.20E+01	No Kr-85 detected		**0.00%**	0.16%
KP323	3.54E+02	Issue with puncturing		**N/A**	0.15%
KP324	3.29E+01	7.40E-02	7%	**0.22% ± 0.02%**	0.16%

4.2 BURNUP CONFIRMATION

Gamma counting was performed for the two NUCO compacts recovered to date. The other fuel specimens recovered could not be measured via gamma counting because they saturated the detector. The Cs-137 and Cs-134 activities were recorded and used to estimate the experimental burnup of the fuel specimens. The experimental burnup was compared to the predicted burnup from the as-built, as-irradiated calculation [4], and the results are reported in Table 1.

The first method (also referred to as method 1) to estimate burnup of the fuel specimen uses the measured Cs-137 activity, as shown in Eq. (1) [11]:

$$BU = \frac{A_{Cs-137}}{\lambda_{Cs-137}\,\gamma_{Cs-137} N_{NM}}\ , \tag{1}$$

where BU is the burnup in percent fission per initial metal atoms (%FIMA), A_{Cs-137} is the measured Cs-137 activity (Bq), λ_{Cs-137} is the Cs-137 decay constant (7.3021 × 10^{10} s^{-1}), γ_{Cs-137} is the Cs-137 fission yield, and N_{HM} is the initial number of heavy metal atoms per fuel specimen. The fission yield was calculated from the number of fissions from U-235 and Pu-239 given by the as-built, as-irradiated calculations.

The second method (also referred to as method 2) to derive experimental burnup uses the linear relationship between burnup and the ratio of the activities of Cs-134 and Cs-137 obtained from the numerical calculations. Figure 6 presents the burnup as a function of the activities of Cs-134 and Cs-137 for the two fuel specimens from the as-built, as-irradiated numerical calculation.

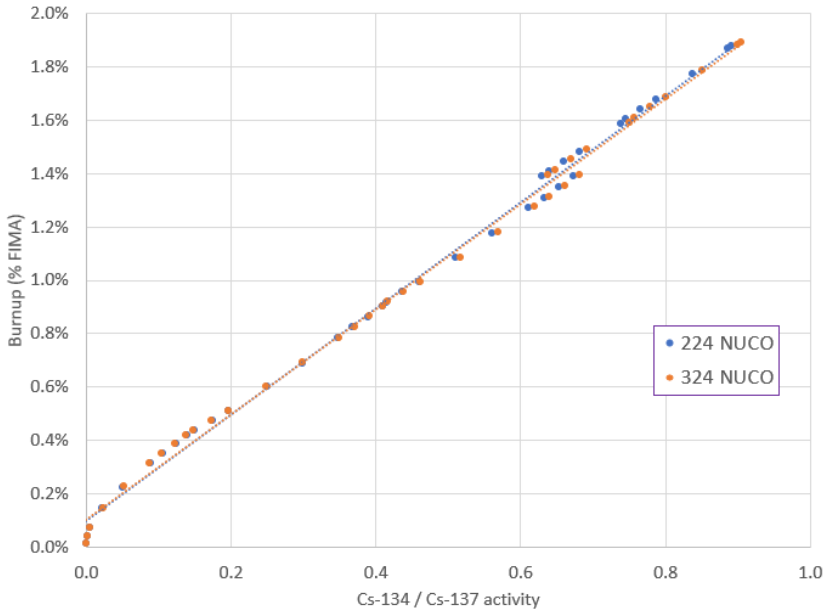

Figure 6. Burnup as a function of the ratio of activities from Cs-134 and Cs-137 from numerical calculations.

Table 4 shows the experimental burnup calculated from method 1 and method 2. Method 1 shows burnup estimates that are slightly over the predicted burnup, whereas method 2 shows results slightly under the predictions. Overall, the two methods agree with the predicted burnup and confirm a burnup of ~2% FIMA for both fuel specimens.

Table 4. Burnup estimates from gamma counting of Cs-137 and Cs-134.

Subcapsule	KP224	KP324
A_{Cs-137} (Bq)	1.97 x 10^7 ± 2.65 x 10^5	1.98 x 10^7 ± 2.66 x 10^5
γ_{Cs-137}	0.05396	0.05400
N_{HM} (atoms)	1.92 × 10^{19} ± 6.07 × 10^{15}	1.92 × 10^{19}± 6.07 × 10^{15}
A_{Cs-134}/ A_{Cs-137}	0.698 ± 0.019	0.680 ± 0.019
Experimental BU (%FIMA) - method 1	**2.59 ± 0.03**	**2.61 ± 0.04**
Experimental BU (%FIMA) - method 2	**1.48 ± 0.04**	**1.45 ± 0.04**
Predicted BU (%FIMA)	**1.90**	**1.89**

5. ADDITIONAL PIE – GAMMA MEASUREMENTS OF SUBCAPSULE COMPONENTS

Gamma counting was performed on the sinks and spacers recovered from the six disassembled capsules. Figure 7 depicts the results of the measurements for the nuclides showing activities above the MDA. For each component, the activity measured for selected fission products is presented as the fraction of the total activity of a given fission product predicted by numerical calculation for the corresponding subcapsule. The fraction of fission products captured by the sinks and the spacers is close to zero, except for Eu-154. The results show a measured Eu-154 activity for the sinks and spacers between 0.5% and 2.5% of the total activity of Eu-154 predicted for the subcapsules. Europium isotopes are often found in HFIR coolant because HFIR control plates contain europium. It is possible that the Eu-154 measured on the sinks and spacers was caused by contamination of the components in the cell, which is often used to cut open experiments that were in contact with the coolant. Release of Eu-154 is also possible from intact and failed TRISO fuel particles [12] and thus cannot be completely discounted at this time.

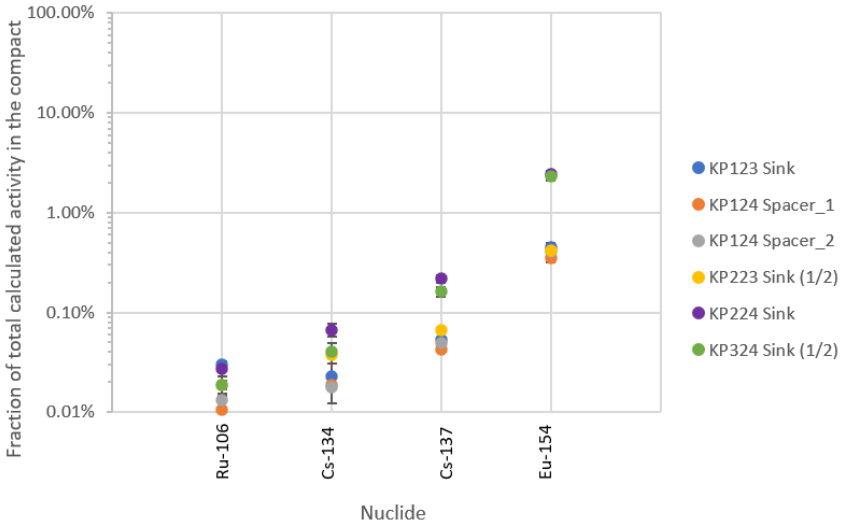

Figure 7. Fractional activity inventory for sinks and spacers recovered to date.

6. FUTURE WORK

The future work for the six disassembled subcapsules (KP224, KP223, KP124, KP123, KP324, KP323) includes a deconsolidation leach burn leach (DLBL) process to determine the number of failed particles per fuel compact. For compact specimens recovered intact, an initial electrolytic deconsolidation/acid leach series will be performed to release the particles from the compact matrix and dissolve any exposed actinides and fission products not contained by the matrix or particle coatings in concentrated nitric acid. Gamma measurements in IMGA and x-ray computed tomography will be performed on selected particles to measure the release of selected fission products, determine the nature of particle failures, and determine the degree of kernel migration/expansion in non-failed particles. A subsequent burn step will be performed by heating in air in a furnace to remove exposed graphitic material via oxidation of the compact matrix carbon and the carbon TRISO coating layers. A final acid leach series will be performed for the "burnback" loose particles to enumerate particle failures with compromised SiC layers and one intact PyC layer. The DLBL process will produce solutions of dissolved exposed actinides and fission products, and the quantification of the dissolved actinides in the leaching solutions will determine the number of failed particles per compact. The DLBL step will be performed at IFEL, and the leaching step will be performed using an experimental setup similar to that represented in Figure 8.

Figure 8. Experimental setup for leaching the fuel specimen.

For the other subcapsules, it is planned to complete puncturing of the subcapsules for FGR measurements, disassembly of the subcapsules, dilatometry on SiC TM to confirm irradiation temperature, and gamma measurements on the fuel compact as well as the sinks and spacers recovered from disassembly.

7. CONCLUSION

This report summarizes the PIE work performed on five MiniFuel targets irradiated in HFIR and containing miniature fuel compacts made of 20 TRISO fuel particles (NUCO, LEUCO, or UO_2 kernels) in a graphite matrix. All the targets were successfully disassembled, and six subcapsules were disassembled to date. Among the six disassembled subcapsules, three fuel compacts were recovered whole, one fuel compact was recovered broken into several pieces of graphite matrix with particles, and two fuel compacts were fully deconsolidated upon disassembly with most of the particles recovered. Dilatometry on SiC passive TM was performed and confirms the predicted irradiation temperature of the components. The results from gamma counting of recovered fuel compacts made it possible to confirm an approximate 2% FIMA experimental burnup for the NUCO fuel compacts. FGR measurements were performed on 13 subcapsules and revealed only one fuel compact with possible fuel particle failure. Table 5 summarizes the PIE performed for each subcapsule. The gray cells in this table correspond with tasks that have not been performed. The future work includes DLBL on the fuel specimens recovered from subcapsule disassembly as well as the

completion of FGR measurements, subcapsule disassembly, components gamma counting, and TM analysis for all the subcapsules of this irradiation testing campaign.

The authors would like to acknowledge David Bryant for his contribution to the subcapsule disassembly, Tash Ulrich, Peter Doyle, and Matt Jones for performing the puncturing of the subcapsules, and Darren Skitt for performing the work in the Irradiated Microsphere Gamma Analyzer (IMGA) cell as well as for gamma counting of the components.

Table 5. Summary of the PIE results collected to date.

Subcapsule ID	Fuel compact	Experimental average SiC layer temperature (°C)	FGR	Subcapsule disassembled	Specimen recovered	Gamma measurement	Experimental Burnup (%FIMA)
KP121	LEUCO		< 0.01%				
KP122	UO_2		0.00%				
KP123	LEUCO	856.1	< 0.02%	X	broken compact (18 particles)	FP sink	N/A
KP124	UO_2	887.8	0.34% ± 0.03%	X	broken compact (19 particles)	Two spacers	N/A
KP125	LEUCO		0.00%				
KP126	UO_2		N/A				
KP221	LEUCO						
KP222	NUCO		< 0.16%				
KP223	LEUCO	577.9	< 0.02%	X	full compact	Half FP sink	N/A
KP224	NUCO	610.7	0.15% ± 0.02%	X	full compact	Compact FP sink	2
KP225	LEUCO		< 0.01%				
KP226	NUCO		0.00%				
KP231	LEUCO						
KP232	LEUCO						
KP233	LEUCO						
KP234	LEUCO						
KP235	LEUCO						
KP236	LEUCO						
KP321	LEUCO						
KP322	NUCO						
KP323	LEUCO	720.4	N/A	X	broken compact	N/A	N/A
KP324	NUCO	695.8	0.22% ± 0.02%	X	full compact	Compact Half FP sink	2
KP325	LEUCO						
KP326	NUCO						
KP331	LEUCO						
KP332	LEUCO						
KP333	LEUCO						
KP334	LEUCO						
KP335	LEUCO						
KP336	LEUCO						

8. REFERENCES

[1] T.J. Gerczak, et al., "Fabrication of MiniFuel Compacts for High-Power Irradiation Testing of TRISO Fuel," ORNL/SPR-2020/1778, Oak Ridge National Laboratory, Oak Ridge, TN, November 2020.

[2] C.M. Petrie, J.R. Burns, A.M Raftery, A.T. Nelson, K.A. Terrani, "Separate effects irradiation testing of miniature fuel specimens," *Journal of Nuclear Materials*, **526** (2019).

[3] R.C. Gallagher, et al., "Analysis and Design of High-Power TRISO Fuel Compact Irradiation in HFIR," ORNL/TM-2020/1658, Oak Ridge National Laboratory, Oak Ridge, TN, June 2021.

[4] J.P. Gorton, et al., "Simulation of a TRISO MiniFuel irradiation experiment with data-informed uncertainty quantification," *Nuclear Engineering and Design*, **404** (2023).

[5] A.G. Le Coq, et al., "Assembly of MiniFuel Targets for Irradiation of TRISO Fuel Compacts in the High Flux Isotope Reactor," ORNL/TM-2021/2057, Oak Ridge National Laboratory, Oak Ridge, TN, July 2021.

[6] A.G. Le Coq, J.P. Gorton, Z.G. Wallen, T.J. Gerczak, K.D. Linton, "Status Report on Irradiation of MiniFuel Targets Bearing TRISO Fuel Compacts," ORNL/TM-2022/2456 Rev. 1, Oak Ridge National Laboratory, Oak Ridge, TN, June 2022.

[7] T.J. Gerczak, et al., "Preirradiation Characterization of MiniFuel Compacts for High-Power Irradiation Testing of TRISO Fuel," ORNL/TM-2021/5, Oak Ridge National Laboratory, Oak Ridge, TN, January 2021.

[8] K. Field, et al., "Evaluation of the Continuous Dilatometer Method of Silicon Carbide Thermometry for Passive Irradiation Temperature Determination," *Nucl. Instrum. Methods Phys Res. B: Beam Interact. Mater. At*. **445**: 46–56 (2019).

[9] J.M. Harp, et al., "Postirradiation examination from separate effects irradiation testing of uranium nitride kernels and coated particles," *Journal of Nuclear Materials*, **554** (2021).

[10] B.J. Lewis, "Fission product release from nuclear fuel by recoil and knockout," Journal of Nuclear Materials, **148** (1987).

[11] J.M. Harp, et al., "An analysis of nuclear fuel burnup in the AGR-1 TRISO fuel experiment using gamma spectrometry, mass spectrometry, and computational simulation techniques", *Nucl. Eng. Des.* **278** (2014) 395–405.

[12] J.D. Stempien, J.D. Hunn, R.N. Morris, T.J. Gerczak, P.A Demkowicz, "AGR-2 TRISO Fuel Post-Irradiation Examination Final Report," INL/EXT-21-64279 Revision 0, Idaho National Laboratory, Idaho Falls, ID, September 2021.